Electronic Supplementary Material (ESI) for Physical Chemistry Chemical Physics.

Supporting Information: First Principles Analysis of Surface Dependent Segregation in Bimetallic Alloys

1. Assessing Simulation Parameters and Slab Design

The chosen DFT parameters are mentioned in the main paper. We performed calculations to determine the effect of using different parameters. Table S1 summarizes these calculations. We first assessed the basis set we used. As Table S1 shows, very different results occur when a single-zeta basis set is used, indicating that such a basis set is likely too small. Therefore we conclude that a double-basis set is adequate for this work. We also tested different exchange correlation functionals. As shown, similar trends are observed when using different functionals, even if the exact energies may be different from each other. As discussed in the main paper, the PBE functional is widely used for surface calculations, so adequately describes surface segregation.

Table S1. Calculated segregation energies (in eV) for a Pt (100) host with select dopants using various exchange correlation functionals and basis sets. The first acronym indicates the exchange correlation functional used (PBE, BLYP, or TPSS), while the second acronym indicates the basis set used (SZ – single zeta, or DZ – double zeta). The main paper presents results using the PBE/DZ parameters.

	Simulation Parameters			
Dopant	PBE/SZ	BLYP/DZ	TPSS/DZ	PBE/DZ
Ir	1.23	0.78	1.39	1.08
Mo	-0.33	1.21	1.84	2.08
Ti	-2.99	1.10	1.48	1.78

We performed calculations to determine the effect of freezing bottom layers versus allowing full relaxation of the layers. We also performed calculations to determine the effect of the number of layers in the slab. Table S2 shows calculated surface energies for the Pt (100) surface. Table S3 shows calculated surface energies for the Pt (111) surface using different number of layers and with and without freezing bottom layer(s). Tables S4 and S5 show surface energies for Pt (110) and (210). The analysis shows that the number of layers did not affect surface energies significantly. Freezing layers did also not have a significant effect on the surface energy. In our work we therefore allowed full relaxation of the slabs and used five layers for the (100) surfaces, 5 layers for the (111) surfaces, 7 layers for the (110) surfaces, and 5 layers for the (210) surfaces. These choices gave slabs that were at least 8 Å thick, to ensure a reasonably thick slab.

Table S2. Calculated surface energies and timing for the Pt (100) surface using different number of layers in the slab and considering freezing of Pt layers.

Number of layers	Frozen Layers	Surface Energy ($eV/Å^2$)
3	None	0.12
4	None	0.11
5	None	0.11
5	Bottom Layer	0.11
6	None	0.10
7	None	0.10
7	Bottom 3 Layers	0.10
8	None	0.10
8	Bottom 4 Layers	0.10

Table S3. Calculated surface energies for the Pt (111) surface using different number of layers in the slab and considering different ways of freezing Pt layers.

Number of layers	Frozen Layers	Surface Energy ($eV/Å^2$)
3	Bottom Layer	0.09
4	None	0.08
5	None	0.08
5	Bottom 2 Layers	0.08
6	None	0.07
7	None	0.07
7	Bottom 4 Layers	0.07
8	Bottom 5 Layers	0.06

Table S4. Calculated surface energies for the Pt (110) surface using different number of layers in the slab.

Layers	Surface energy (eV/A2)
4	0.12
5	0.12
6	0.12
6-bottom layer frozen	0.12
7	0.12
7-bottom layer frozen	0.12

Table S5. Calculated surface energies for the Pt (210) surface using different number of layers in the slab.

Number of layers	Surface energy eV(A2)
4	0.12
5	0.12
6	0.12
7	0.12

We also performed segregation energy calculations using a 5-layer Pt (111) surface and Ag as a dopant with different number of frozen layers, as given in Table S6. Again these results verify that a fully relaxed 5 layer slab is sufficient for this work.

Table S6. Calculated segregation energies for the Pt (111) surface considering freezing different number of layers with Ag as a dopant. As it is evident, freezing does not have much effect on the segregation energy values. Since non-freezing needed the least computation time, while giving accurate results, we did not freeze any layer throughout our calculations.

Number of frozen layers	Segregation energy
0	-0.51
1	-0.51
2	-0.50
3	-0.48

We also determined whether the sizes of our simulation cells were large enough so that any errors related to simulation cell size were minimal. The surface cells we used for Pt had lattice lengths between 15.8 and 17.7 Å. By increasing the surface slab size, errors related to k-points would be minimized, as well as energies related to dopant-dopant interactions. Table S7 shows the results of such calculations, were we modeled for Pt (100) a larger cell compared to the surface cell reported in the main text. The results show that increasing the surface cell size (from 16.8 to 19.6 Å) does not affect segregation energies significantly.

Table S7. Calculated segregation energies (in eV) for the Pt (100) surface comparing (7x7) and (6x6) surface cells.

Dopant	(7x7) Surface Cell	(6x6) Surface Cell
Cr	1.24	1.26
Ru	1.22	1.30
Ta	2.05	2.13

In Figure S1 we show the different dopant positions in the surface slabs.

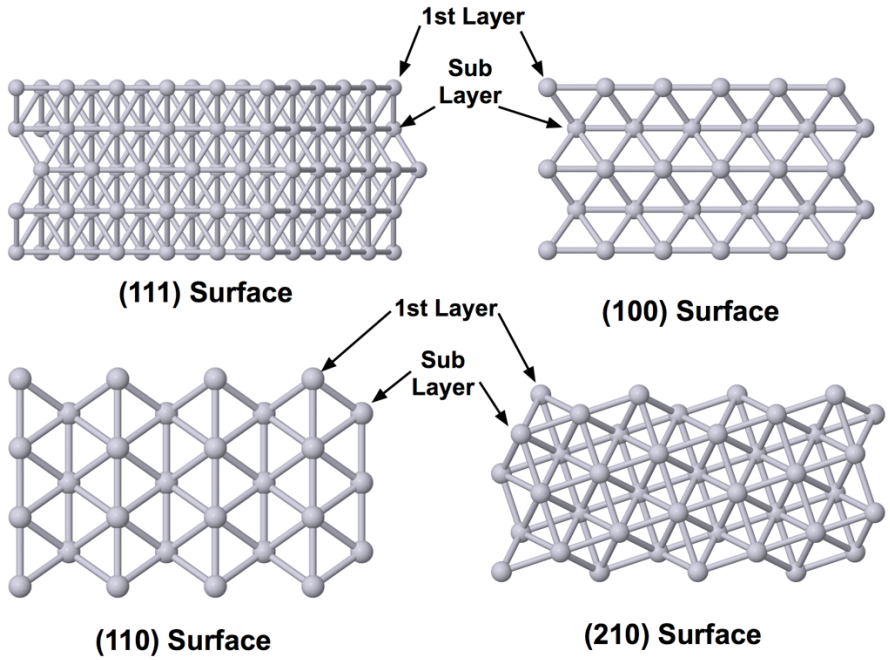

Figure S1. Indicated positions of dopant metals that were modeled in the various surfaces.

2. Calculated Segregation Energies

Segregation energies ($E_{seg-1-bulk}$) in (100) surfaces of Pt, Pd, Ir, and Rh are depicted in Figure S2. Segregation energies ($E_{seg-1-bulk}$) for (110) and (210) surfaces of Pt, Pd, Ir, and Rh are also shown in Figures S3 and S4 respectively. As was explained in the main text for (111)

surfaces and as also evident from Figure S5, Ir has the most negative segregation energies, while Pt has the most positive segregation energies.

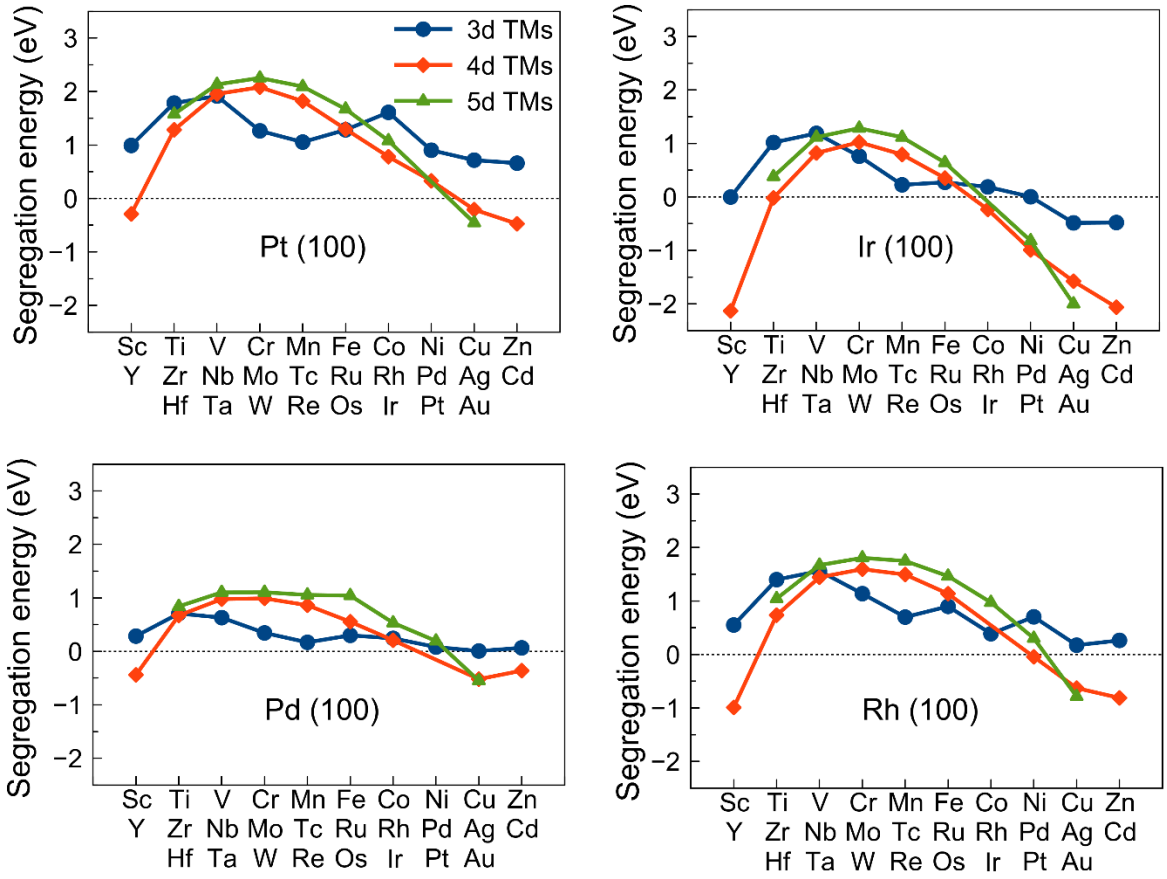

Figure S2. Calculated segregation energies within (100) surfaces of Pt, Pd, Ir, and Rh.

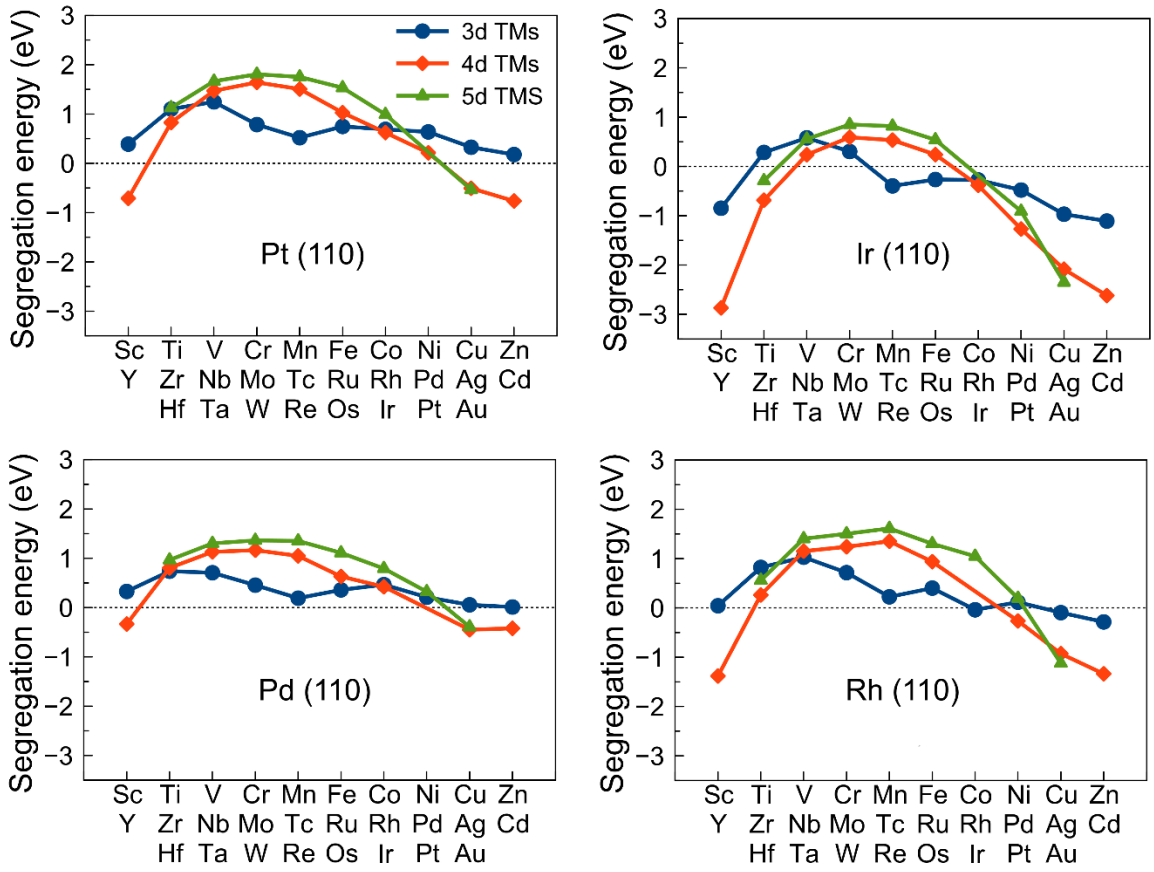

Figure S3. Calculated segregation energies within (110) surfaces of Pt, Pd, Ir, and Rh.

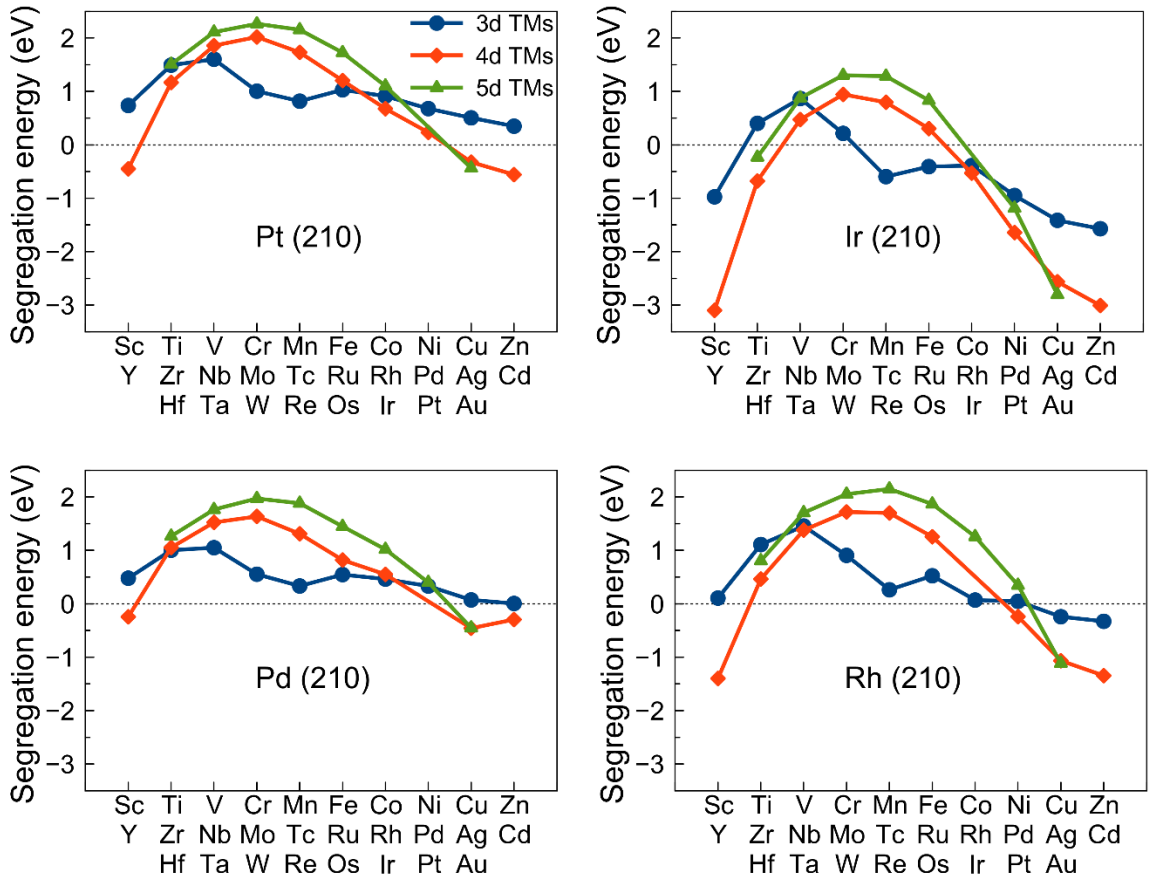

Figure S4. Calculated segregation energies within (210) surfaces of Pt, Pd, Ir, and Rh.

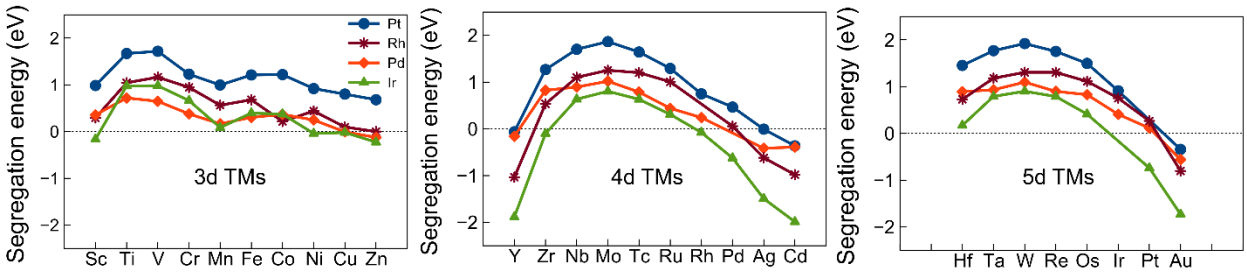

Figure S5. Comparison between (111) surfaces of Pt, Pd, Ir, and Rh as hosts. The segregation energies follow this trend: Pt > Rh > Pd > Ir.

3. Models for Predicting Surface Segregation

We were interested to see if there is a correlation between d-band properties of different surfaces of host metals with segregation energy values. We calculated d-band width, d-band filling, and d-band center for (111), (100), (110), and (210) of our host metals. To investigate such a correlation, we considered V as the dopant and Pt as the host as we observed the trend of (100)>(111)>(210)>(110). Figure S6 shows d-band width versus segregation energy, d-band filling versus segregation energy, and d-band center versus segregation energy. As it can be seen there is no obvious correlation between d-band properties of the host and segregation energy values. Later we showed comparing equations S.8 and S.13 that d-band properties of the host played a slight role in predicting segregation energies of dopants in our host metals. In other words, adding a term which takes into account d-band properties of the host, improved the adjusted R^2 only by 0.01.

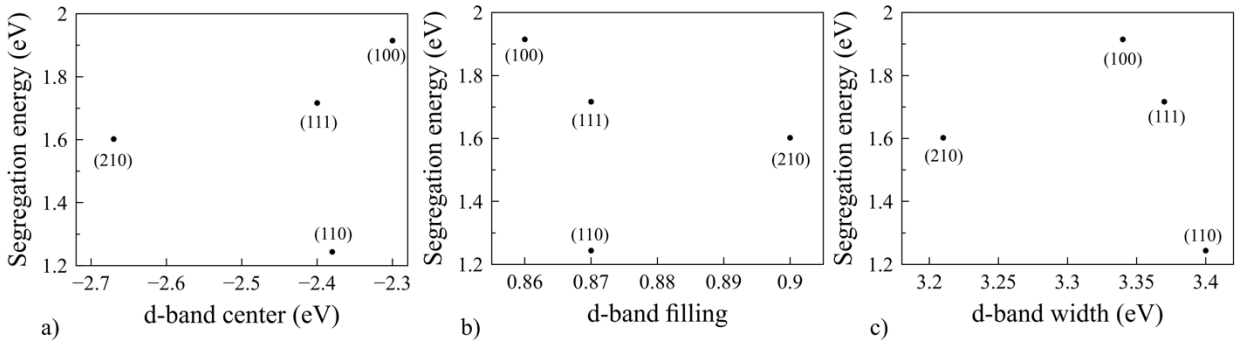

Figure S6. Plot of segregation energy of Vanadium (V) as a dopant in (111), (100), (110), and (210) surfaces of Pt along with d-band properties of pure surfaces of Pt (without dopant). a) d-band center and segregation energy, b) d-band filling and segregation energy, and c) d-band width and segregation energy comparison for different surfaces of Pt. As it can be observed, there is not a linear correlation between different surfaces of Pt and d-band properties of the pure surfaces.

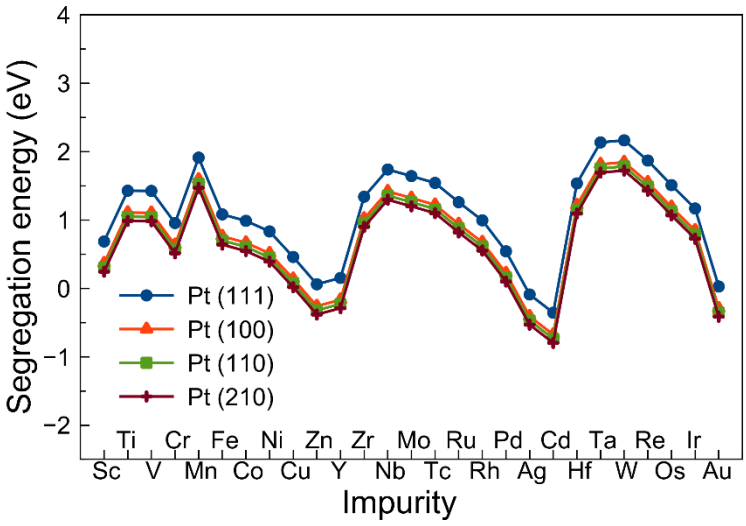

Figure S7. Modified Yu et al.'s model segregation data.

Yu et al[1]. developed a model for segregation energy based on difference in surface energy, elastic energy, and heat of solution of the impurity and the host metal. Their model can be written as the following:

$$E_{seg} = C_1 \Delta E_{surf} + C_2 \Delta E_{elast} + C_3 E_{sol} \quad \text{(S.1)}$$

They explained that based on previous literature, the ΔE_{elast} term can be written as the following:

$$\Delta E_{elast} \propto \left[\left(\frac{r_B}{r_A}\right)^3 - 1\right]^2 r_A^3 \quad \text{(S.2)}$$

In this equation B represents the impurity. r_B and r_A denote the Van der Waals radii of the impurity and the host respectively. The heat of solution can be calculated by the following formula:

$$E_{sol} = E_{A_nB_m} - nE_A - mE_B \quad \text{(S.3)}$$

$E_{A_nB_m}$ is the total energy of the $E_{A_nB_m}$ unit cell that contains n number of A atoms and m number of B atoms. E_A and E_B are the total energy of one A or B atom in the bulk. All these energies are calculated with DFT. Figure S7 shows a comparison of different segregation energies calculating using Yu et al.'s model for Pt, after refitting the parameters to our data.

In order for us to develop a model to predict surface dependent segregation energy, we considered different parameters which could potentially affect surface segregation energies

including: d-band width and d-occupation number of the host, d-band width and d-occupation number of the dopant, geometric mean of d-band width of the host and the dopant, electronegativity of the transition metals used as dopants, Ionization potential, electron affinity, number of d-electrons, cohesive energy, polarizability, atomic and group number of dopants involved, work function, surface energy, surface energy difference between host and the dopant, Wigner-Seitz radius, Van Der Waals radius, the $\left[\left(\frac{r_B}{r_A}\right)^3 - 1\right]^2 r_A^3$ term (taken from Yu et al.[1] which is correlated with elastic energy) using Wigner-Seitz radii of host and dopant (referred to WS correlation), the $\left[\left(\frac{r_B}{r_A}\right)^3 - 1\right]^2 r_A^3$ term (taken from Yu et al.[1]), this time using Van der Waals radii of host and dopant (referred to VDW correlation), the $\left[1 - \left(\frac{Z_b}{Z_s}\right)^{\frac{1}{2}}\right]$ term named coordination contribution and the $\{W^A N_A(10 - N_A) - W^{B\to A} N_B(10 - N_B)\}$ term named as bandwidth contribution. (both taken from Ruban et al[2]).

We then developed different linear and non-linear regression models to investigate which terms to use in our model. While making different models, we tried different combination of parameters and whichever gave the best adjusted R^2 (which helps correct overfitting) was used. After trying out multiple models, we proposed Equation S.4 to predict surface dependent segregation energies. In our Equation S.4, we used the terms implemented in Ruban et al[2] (coordination numbers and d-band properties) and Yu et al[1] models (surface energy and VDW correlation).

Our model we developed to predict surface segregation is as follows:

$$E_{segregation}^{B\to A} = 1.93 - 0.04W^B - 0.21N_B + 0.63\left(E_{surface}^B - E_{surface}^A\right) - 0.53 \left[\left(\frac{r_B}{r_A}\right)^3 - 1\right]^2 r_A^3 - 0.62\left[1 - \left(\frac{Z_b}{Z_s}\right)^{\frac{1}{2}}\right] \quad \text{(S.4)}$$

The parameters implemented in our model (Equation 3) are $\beta_0 = 1.93, \beta_1 = -0.04, \beta_2 = -0.21, \beta_3 = 0.63, \beta_4 = -0.53, \beta_5 = -0.62$. In the above equation, $E_{segregation}^{B\to A}$ denotes the segregation energy of dopant B in the host of A. W^B is the d-bandwidth of dopant, , N_B is the d-occupation number of the dopant, $E_{surface}^A$ and $E_{surface}^B$ are surface energies of the bare metals, r_A and r_B are Van der Waals radii, and Z_b and Z_s are coordination numbers. In all cases A refers

to the host and B represents the dopant. The $\left[\left(\frac{r_B}{r_A}\right)^3 - 1\right]^2 r_A^3$ term is associated with elastic energy release and was inspired by Yu et al.[1] The variables $\left[1 - \left(\frac{Z_b}{Z_s}\right)^{\frac{1}{2}}\right]$, W^B, and N_B are inspired by Ruban et al.[2]. The values in Equation (S.4) for the dopant (B) are summarized in Table S8. The values of d-band width and d-band filling in Table S8 are taken from Table 1 in the Brejnak and Modrak paper[3]. The values of surface energy (for dopants) and van der Waals radius are taken from Table 2 in Yu et al.'s paper[1]. Surface energy, d-band width, and d-band filling of the host metal were calculated with DFT. For calculating d-band width and d-band filling, we used Equations 2 and 3 from Xu and Kitchin's paper[4]. In order to calculate d-band width, first we calculated d-band center using Equation 1 from their paper[4]. These equations are listed as equations S.5-S.7:

$$E_l = \frac{\int \rho E dE}{\int \rho dE} \qquad \text{(S.5)} \qquad W_l^2 = \frac{\int \rho (E - E_l)^2 dE}{\int \rho dE} \qquad \text{(S.6)} \qquad f_l = \frac{\int_{-\infty}^{E_f} \rho dE}{\int_{-\infty}^{\infty} \rho dE} \qquad \text{(S.7)}$$

In Equations S.5-S.6, E_l denotes the d-band center corresponding to the state l and is computed based on the first moment of the projected density of states about the Fermi level (E_f). W_l is calculated based on square root of second moment of the projected density of states about the d-band center; and the fractional d-band filling is calculated based on the integral over states up to Fermi level divided by the integral over all states.

In order to calculate surface energies for (111), (100), (110), and (210) of our host metals, we used the following formula[5]:

$$E_{surface} = \frac{E_{tot}^{slab} - N E_{tot}^{bulk}}{2A} \qquad \text{(S.8)}$$

In the above formula $E_{surface}$ is the calculated surface energy, E_{tot}^{slab} is the total energy of the slab containing N number of atoms, E_{tot}^{bulk} is the energy per atom of the bulk system, A is the surface area of the slab, and the factor 1/2 takes into account the presence of two equivalent surfaces of the slab.

We also used the term associated with d-band width and d-band filling of the host and impurity ($W^A N_A(10 - N_A) - W^{B \to A} N_B(10 - N_B)$) as proposed by Ruban et al[2]. Based on our analysis, adding this term did not increase the accuracy of our model considerably. Using the

following model, which adds these d-band properties of the host and impurity, results in a R^2 value of 0.79, adjusted R^2 of 0.78, and $RMSE$ of 0.42 eV which is not much of an improvement compared to our original model:

$$E_{segregation}^{B\to A} = 1.56 - 0.09W^B - 0.15N_B - 0.006\{W^A N_A(10-N_A) - W^{B\to A}N_B(10-N_B)\} + 0.60\left(E_{surface}^A - E_{surface}^B\right) - 0.41\left[\left(\frac{r_B}{r_A}\right)^3 - 1\right]^2 r_A^3 - 0.59\left[1 - \left(\frac{Z_b}{Z_s}\right)^{\frac{1}{2}}\right] \quad \text{(S.9)}$$

Tables S8 and S9 shows the values we used for fitting our model.

Table S8. Dopant data implemented in Equation 3. d-band width and d-band-filling are taken from Brejnak and Modrak[3]. Surface energy and ban der Waals radius are taken from Yu et al[1].

Transition metal	d-band width(eV)	d-band-filling	Surface energy (J/m^2)	van der Waals radius (A)
Sc	5.1	1.76	1.275	2.61
Ti	5.8	2.90	2.1	2.39
V	6.1	3.98	2.55	2.29
Cr	6.0	4.96	2.3	2.25
Mn	5.0	6.02	1.6	2.24
Fe	4.5	6.93	2.475	2.23
Co	4.1	7.87	2.55	2.23
Ni	3.7	8.97	2.45	2.22
Cu	2.8	9.91	1.825	2.26
Y	7.4	1.68	1.13	2.71
Zr	8.9	2.96	2	2.54
Nb	10.0	4.10	2.7	2.43
Mo	10.0	5.07	3	2.39
Tc	9.5	6.23	3.15	2.36
Ru	8.6	7.24	3.05	2.34
Rh	7.1	7.99	2.7	2.34
Pd	5.5	8.96	2.05	2.37
Ag	3.6	10.00	1.25	2.43
Hf	10.2	2.69	2.15	2.53
Ta	11.6	3.78	3.15	2.43
W	11.7	4.73	3.675	2.39
Re	11.4	5.73	3.6	2.37
Os	10.7	6.70	3.45	2.35
Ir	9.2	7.65	3	2.36
Pt	7.3	8.74	2.475	2.39
Au	5.3	9.89	1.5	2.43

Table S9. DFT based data for host metals implemented in Equation 3. d-band widths, d-band fillings, and surface energies were calculated with Equations (S.6), (S.7), and (S.8) respectively.

Host	d-band width (eV)	d-band filling	Surface energy (J/m^2)	Coordination number at the surface	Coordination number in the bulk
Pt (111)	3.37	0.87	1.332	9	12
Pt (100)	3.34	0.86	1.773	8	12
Pt (110)	3.40	0.87	1.857	7	12
Pt (210)	3.21	0.90	1.941	6	12
Ir (111)	3.75	0.76	2.624	9	12
Ir (100)	3.74	0.76	3.096	8	12
Ir (110)	3.77	0.76	3.133	7	12
Ir (210)	3.62	0.76	3.226	6	12
Pd (111)	2.52	0.89	1.404	9	12
Pd (100)	2.51	0.90	1.616	8	12
Pd (110)	2.50	0.89	1.673	7	12
Pd (210)	2.48	0.89	1.707	6	12
Rh (111)	2.89	0.79	2.336	9	12
Rh (100)	2.88	0.79	2.506	8	12
Rh (110)	2.89	0.78	2.534	7	12
Rh (210)	2.83	0.79	2.574	6	12

Comparison between segregation energies calculated with DFT and our model for (111), (100), (110), and (210) surfaces of Ir, Pd, and Rh are shown in Figures S8, S9, and S10 respectively. Our model follows segregation behavior very well, especially for the Ir and Rh surfaces.

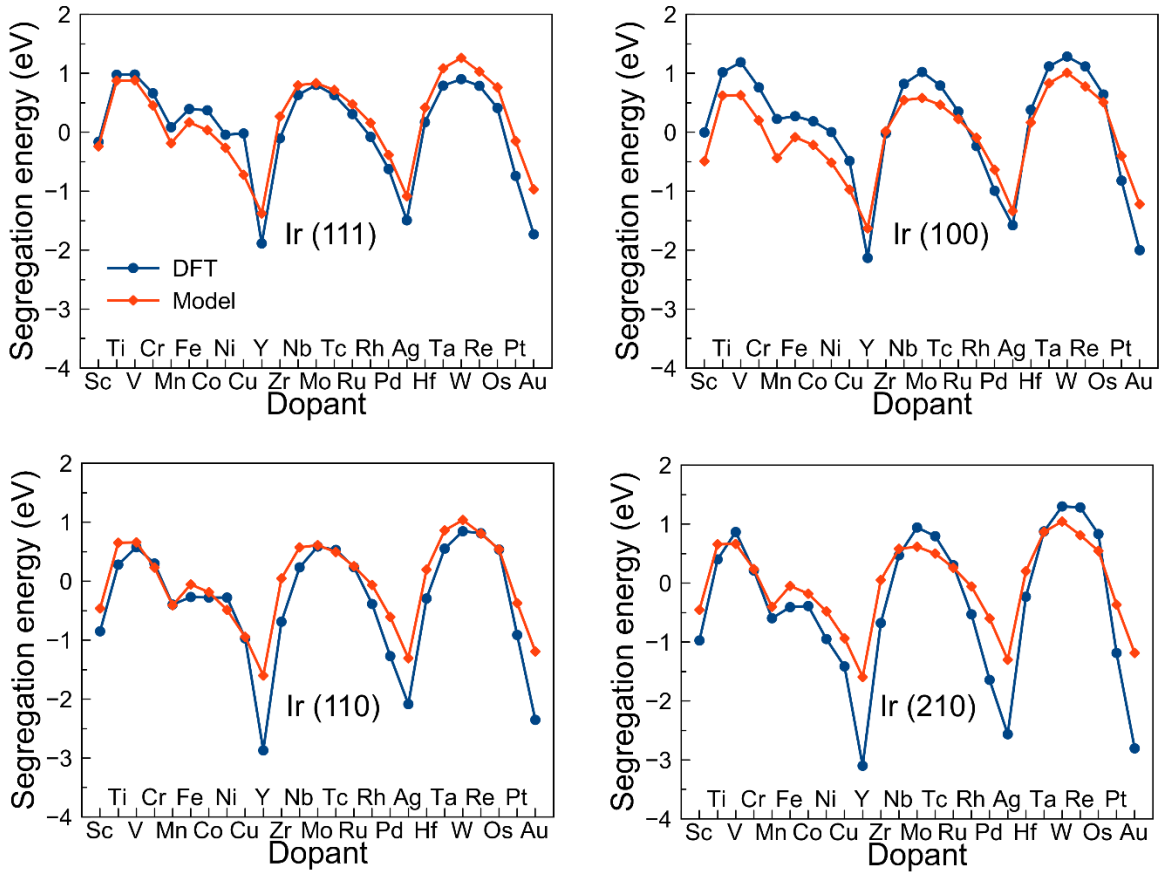

Figure S8. Comparison of segregation energies for dopants in (111), (100), (110), and (210) surfaces of Ir obtained with DFT and our model.

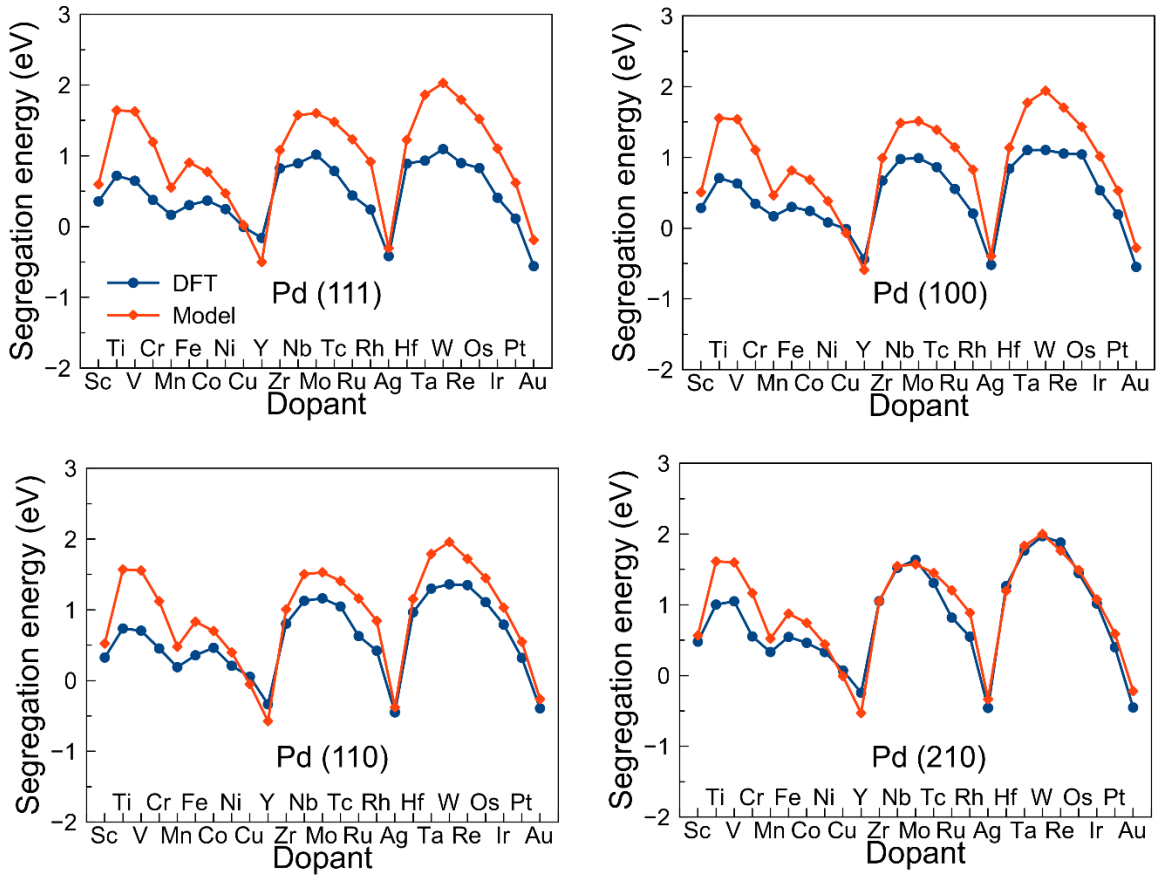

Figure S9. Comparison of segregation energies for dopants in (111), (100), (110), and (210) surfaces of Pd obtained with DFT and our model.

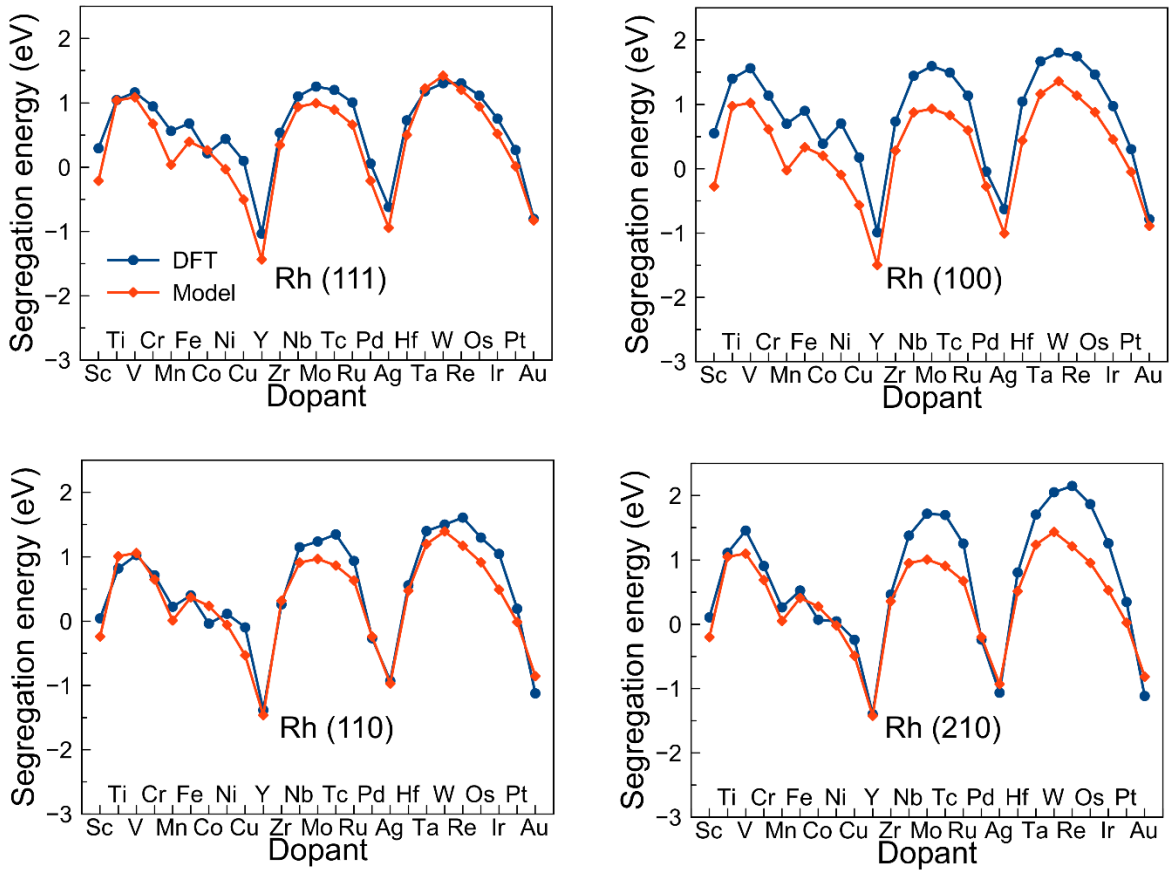

Figure S10. Comparison of segregation energies for dopants in (111), (100), (110), and (210) surfaces of Rh obtained with DFT and our model.

We also calculated segregation energies using our model (Equation S.4) for the Pt (211) surface. This surface was not used in the fitting of the model so presents an opportunity to test how robust our model is. Table S10 shows that this model works well in predicting segregation energies for surfaces outside our fitting data set.

Table S10. Calculated segregation energies (in eV) using DFT and the model we developed. Results are for the Pt (211) surface, which was not used to fit our model. As shown, the model predicts the segregation energies well.

Dopant	DFT	Our Model
Ir	1.03	1.01
Mo	2.20	1.52
Ru	1.32	1.13
Cr	1.31	1.06

References

1. Yu, Y. L.; Xiao, W.; Wang, J. W.; Wang, L. G., Understanding the surface segregation behavior of transition metals on Ni(111): a first-principles study. *Phys Chem Chem Phys* **2016,** *18* (38), 26616-26622.
2. Ruban, A. V.; Skriver, H. L.; Norskov, J. K., Surface segregation energies in transition-metal alloys. *Phys Rev B* **1999,** *59* (24), 15990-16000.
3. Brejnak, M.; Modrak, P., Electronic theory of surface segregation for dilute transition metal alloys: predictions based on rigid-band-like approach. *Surface Science* **1991,** *247* (2-3), 215-221.
4. Xu, Z.; Kitchin, J. R., Relationships between the surface electronic and chemical properties of doped 4d and 5d late transition metal dioxides. *The Journal of chemical physics* **2015,** *142* (10), 104703.
5. Michaelides, A.; Scheffler, M., An introduction to the theory of metal surfaces. *Textbook of Surface and Interface Science* **2010,** *1*.